Final Technical Report

Development of a Photo Electron Emission Microscopy-Free Electron Laser System (PEEM-FEL) for Studies of the Dynamics of Surface Processing and Epitaxial Growth

Supported under Grant #NOOO14-95-1-1141
Office of the Chief of Naval Research
Report for the Period of May 1995-April 1998

Robert J. Nemanich, Harald W. Ade and Robert F. Davis*
c/o Physics Department,
and
*Materials Science and Engineering Department
North Carolina State University
Campus Box 8202
Raleigh, NC 27695-8202

July, 1998

REPORT DOCUMENTATION PAGE

Form Approved
OMB No. 0704-0188

1. AGENCY USE ONLY *(Leave blank)*	2. REPORT DATE	3. REPORT TYPE AND DATES COVERED
	July 27, 1998	Final Technical May 1995-April 1998

4. TITLE AND SUBTITLE
Development of a Photo Electron Emission Microscopy-Free Electron Laser System (PEEM-FEL) for Studies of the Dynamics of Surface Processing and epitaxial Growth

5. FUNDING NUMBERS

6. AUTHOR(S)
Robert J. Nemanich, Harald W. Ade and Robert F. Davis

7. PERFORMING ORGANIZATION NAME(S) AND ADDRESS(ES)
North Carolina State University
Hillsborough Street
Raleigh, NC 27695-8202

8. PERFORMING ORGANIZATION REPORT NUMBER
NOOO14-95-1-1141

9. SPONSORING/MONITORING AGENCY NAMES(S) AND ADDRESS(ES)
Sponsoring: ONR, 800 N. Quincy, Arling, VA 22217-5660
Monitoring: Administrative Contracting Officer, Office of Naval Research Regional Office Atlanta, 101 Marietta Tower, Suite 2805
101 Marietta Street, Atlanta, GA 30323-6145

10. SPONSORING/MONITORING AGENCY REPORT NUMBER

11. SUPPLEMENTARY NOTES

12a. DISTRIBUTION/AVAILABILITY STATEMENT
Approved for Public Release; Distribution Unlimited

12b. DISTRIBUTION CODE

13. ABSTRACT ***(Maximum 200 words)***

This program has successfully addressed the development of a high resolution photo electron emission microscopy (PEEM) system with in situ surface preparation capabilities to be combined with the UV free electron laser at Duke University. This unique combination of PEEM at a UV FEL allows in situ, real time, high resolution surface microscopy of the dynamics of surface processing and epitaxial growth. The PEEM system was developed by Elmitech to the specifications of this project. The system specified a lateral resolution of less than 10nm, and a resolution of ~12nm has been verified. A close working arrangement has been established with the Duke University Free Electron Laser Laboratory for the operation at the UV-FEL, and the PEEM is now being used with the UV FEL. Results have been obtained for the following semiconductor experiments: FEL-PEEM real time growth studies of the formation of silicide islands on Si, FEL-PEEM of diamond surfaces vs. in situ annealing, PEEM of GaN pyramid electron emission arrays. Moreover, these initial measurements have demonstrated real time observation of complex dynamical processes on semiconductor surfaces.

14. SUBJECT TERMS
Photo electron emission microscopy, surface properties epitaxial film growth

15. NUMBER OF PAGES
26

16. PRICE CODE

17. SECURITY CLASSIFICATION OF REPORT	18. SECURITY CLASSIFICATION OF THIS PAGE	19. SECURITY CLASSIFICATION OF ABSTRACT	20. LIMITATION OF ABSTRACT
UNCLAS	UNCLAS	UNCLAS	SAR

Submitted to Surface Review and Letters

A FREE ELECTRON LASER – PHOTOEMISSION ELECTRON MICROSCOPE SYSTEM (FEL-PEEM)

H. Ade*, W. Yang*, S. L. English**, J. Hartman**, R. F. Davis**, R. J. Nemanich*, V. N. Litvinenko***, I. V. Pinayev***, Y. Wu*** and J. M. J. Madey***

*Department of Physics and **Engineering, NCSU, Raleigh, NC 27695.
*** FEL Laboratory, Department of Physics, Duke University, Durham, NC 27708.

We report first results from our effort to couple a high resolution Photoemission Electron Microscope (PEEM) to the OK-4 Ultra Violet Free Electron Laser at Duke University (OK-4/Duke UV FEL). The OK-4/Duke UV FEL is a high intensity source of tunable monochromatic photons in the 3-10 eV energy range. This tunability is unique and allows us to operate near the photoemission threshold of any samples and thus maximize sample contrast while keeping chromatic aberrations in the PEEM minimal. We have recorded first images from a variety of samples using spontaneous radiation from the OK-4/Duke UV FEL in the photon energy range of 4.0 to 6.5 eV. Due to different photothreshold emission from different sample areas, emission from these areas could be turned on (or off) selectively. We have also observed relative intensity reversal with changes in photon energy which are interpreted as density of state contrast. Usable image quality has been achieved, even though the output power of the FEL in spontaneous emission mode was several orders of magnitude lower than the anticipated full laser power. The PEEM has achieved a spatial resolution of 12 nm.

I. Introduction and background

Low Energy Electron Microscopy (LEEM) and Photoemission Electron Microscopy (PEEM) have gained prominence during the last decade due to their ability to provide *real time* imaging of surfaces with nanometer lateral resolution and a large field of view. In addition, the contrast mechanisms employed provide structural (LEEM) as well as indirect chemical information (PEEM, work-function contrast) information. These attributes make LEEM and PEEM ideally suited for dynamical studies of surfaces, and numerous efforts are underway to utilize the power of LEEM and PEEM to study a wide variety of scientific issues.

LEEM and PEEM are microscopy techniques which are based on the emission of electrons from surfaces which are subsequently imaged using electron optics [1]. In LEEM, low energy diffracted electrons are utilized [2], while in PEEM secondary and primary photoelectrons created by UV light are used. LEEM routinely reaches a spatial resolution of 10 nm, while PEEM with laboratory based sources has reached this level of spatial resolution only in isolated cases due to intensity limitations. There are only a limited number of samples with photothresholds matched to the output of laboratory sources[3,4]. Since both techniques use similar electron optics to provide the spatial resolution, PEEM operation is readily available in a LEEM if the sample can be illuminated with a UV light source. However, the operation of a LEEM requires the separation of an incoming electron beam from the backscattered/diffracted electron beam into two electron beams. Typically, two separate lens columns are utilized which are at an angle with respect to each other[2,5,6]. This complicates the electron optics and operation of a LEEM in comparison to an instrument that provides only PEEM. The latter instrument can consist of a single, straight electron beam column, which simplifies operation and maintenance.

While most efforts to date involving material science have utilized a LEEM[6-10], we conceived and operate an optimized PEEM which offers several complementary aspects. The principle utility of our PEEM arises from two attributes: a) we couple well understood and relatively simple electron optics to the most powerful tunable UV source available (the OK-4/Duke UV FEL), b) we explore contrast mechanisms complementary to that of LEEM.

Our own interest to utilize emission microscopy is not motivated by the ultimate spatial resolution achievable (which can be exceeded by other probes, such as AFM, STM, etc.) but by the physical mechanisms that provide contrast in a PEEM (and its simplicity when compared to a LEEM). With PEEM it is possible to image the spatial distribution and time dependance of material composition and structure indirectly through changes in surface work function and electron affinity, changes in valence band density of states, or changes of low lying core levels [3,11]. In addition, a PEEM can operate over a wide temperature (up to 2000K) and pressure range (10^{-5} - 10^{-11} torr). These advantages have been most elegantly demonstrated in a series of experiments by Ertl's group from the Fritz Haber Institute of Berlin, who has imaged the spatial and temporal variations of chemical domains formed during catalytic reactions on metal surfaces [12,13]. However, the full exploitation of PEEM capabilities has so far been limited by the relatively low intensity of conventional laboratory UV sources, and the lack of energy tunability both of which restrict the range of samples that can be investigated. These limitations will be removed by operating a PEEM with the tunable, high intensity OK-4/Duke UV FEL.

The OK-4/Duke UV FEL source spans the energy range of 3-10 eV. This energy range is most effective for low-energy emission microscopy. We will exploit the tunability to provide maximum valence band, electron affinity, or work function contrast. For example, optimized workfunction contrast in a PEEM is achieved by adjusting the photon energy to be in-between the work function of various surface features. This would then result in regions on the sample that would not emit electrons at all while other regions would emit electrons, a situation that results in very high contrast images. In addition, the electrons that do emerge from the surface have very low energies and therefore a small energy spread. This keeps chromatic aberrations of the electron optics small without resorting to an energy filter and the electron energy spread will not degrade the spatial resolution.

In the following sections we will describe the hardware of our PEEM, the OK-4/Duke UV FEL facility and some of our first applications.

II. FEL-PEEM

II. 1. High resolution PEEM.

A custom PEEM system was purchased from Elmitec. It employs the same objective lens that is utilized in the successful and productive microscopes developed by Bauer's group, with a nominal resolution of about 10 nm. The lens column and part of the object chamber are displayed in Fig. 1. The electron optics is rather conventional by now. It consists of a magnetic objective lens, a transfer lens, a field lens, an intermediate lens and a double-gap projector, as well as stigmators. The optics and lenses are essentially the same as in the spectroscopic LEEM described by Veneklasen[5], but for the illuminating column, the separator and the energy analyzer in the latter instrument. Contrast apertures 50, 70 and 100 μm in size can be inserted in a conjugated diffraction plane of the objective. The intermediate lens will allow the PEEM to be upgraded to an energy filtered X-ray PEEM in the future. A conjugate diffraction plane, rather than an image plane can than be projected at the entrance plane of the energy filter. The energy filter would be inserted in between the intermediate lens and the projector lens. Total magnification of 1000X can be achieved at the location of the image intensifier consisting of a dual-channel plate, a phosphor screen, and fiber optic phase plate arrangement from Galileo. The lens column is differentially pumped to allow high-pressure operation of the PEEM while protecting the image intensifier. Our object chamber has 6 ports for various sources for *in-situ* growth. We can evaporate metals and will install the necessary sources for growth of thin layers of various wide band gap materials including III-nitrides. We have also installed a Reflection High Energy Electron

Diffraction (RHEED) system to monitor the surface structure and its change during growth. Unfortunately, the RHEED and the PEEM can not be simultaneously operated. Nevertheless, the RHEED allows us to monitor the average surface structure without a sample transfer, or even without moving the sample at all. The sample holder has been modified to be compatible with the RHEED in the nominal PEEM sample location. The sample manipulator and sample cartridges are essentially those developed by Bauer's group.

The growth capabilities in the FEL-PEEM object chamber are limited to thin layers. In order to avoid having to transport samples through air or poor vacuum for preparation and pre-characterization, we will couple the PEEM via a sample transport system to a sophisticated Molecular Beam Epitaxial (MBE) growth chamber that is able to prepare substrate films of various composition. Complementary surface characterization techniques such as Auger electron spectroscopy (AES) will also be available in the MBE growth chamber. The design has been completed and we are in the process of final assembly of the MBE growth chamber. The MBE will be coupled to the FEL-PEEM in the near future in an expanded laboratory.

II. 1. OK-4/Duke UV FEL

The OK-4/Duke storage ring UV FEL is a special source of radiation capable of generating a broad range (IR to soft X-rays) of spontaneous emission, as well as coherent UV radiation. The 1 GeV Duke storage ring is dedicated to drive the OK-4 FEL which is located in the South straight section of the ring. A schematic of the facility is shown in Fig.2. The main parameters of this facility are published elsewhere [14]. The OK-4 FEL is an optical klystron comprising two plane electromagnetic wigglers and a buncher. The wavelength of the OK-4 spontaneous radiation can be adjusted from 0.6 eV to 1 keV by adjusting the magnetic field strength of the wigglers and/or the energy of the electron beam from 0.25 to 1 GeV. The linewidth of the radiation from the OK-4 wiggler is typically better than 1%. The OK-4/Duke FEL has also demonstrated lasing with a tunable photon energy from 3 to 5.48 eV [15]. This upper limit, 5.48 eV is the highest photon energy achieved with FELs to date. The typical linewidth during lasing operation of the OK-4/Duke UV FEL is about $\Delta E/E=10^{-4}$. The tuning range for a given set of UV multilayer mirrors is about 18-25% around the central energy. Fig. 3 shows the predicted performance of the OK-4/Duke UV FEL for an average beam current of 100 mA, a current that has been already achieved. Compared to the other UV lasers, the greatest advantage of the OK-4 FEL for the FEL-PEEM is its tunability, and its potential to provide beams of higher photon energies in the future.

Here we summarize the OK-4/Duke UV FEL experimental conditions which have been used for the reported experiments. We have used spontaneous radiation of the fundamental harmonic from the OK-4 wigglers with tunable photon in the 3-10 eV range. The spontaneous wiggler radiation is only partially coherent and has a spectral resolution depending on the geometry. The energy of photons depends also on the observation angle and therefore on the collimation of the used beam. We have used a linewidth $\Delta E/E$ of about 3%, which corresponds to an energy width of less than 200 meV. A typical measured spectrum of spontaneous radiation used for our experiments is shown in Fig. 4. The first experiments were performed using spontaneous radiation generated by a few milliamperes of stored electron beam current. This provided about 30 μW of average power at the sample location.

In the future, the OK-4/Duke UV FEL will provide an average power of at least 1 W in the energy range of interest. At the location of the PEEM this corresponds to a power density of 1 kW/cm^2 if the beam is refocused to a spot size of about 100 μm vertically by 1 mm horizontally on the sample. This size would be matched in the vertical to a field of view at low PEEM magnification. Even with a photo-yield as low as 0.1%, 1 W of power results in a photoelectron current of 1 mA, which corresponds to a current density at the sample of 100 $A/(\mu m)^2$. In order to provide a reference point, we compare these numbers to a LEEM that is operated with a current of about 10 nA into a 100 μm spot on the sample. This corresponds to a current density of 1 $A/(\mu m)^2$. The photoelectron current density necessary for high spatial resolution performance of the FEL-PEEM is actually smaller than current densities required in a LEEM operated in "dark-field" mode. In LEEM dark field mode, only a subset of the electrons emanating from the surface are used for image formation. Hence, the current density in the FEL-PEEM should provide enough signal to allow imaging at 10 nm spatial resolution with 1% of noise in a single video frame 1/30 of a second in duration. However, the OK-4 output is pulsed with a duty-cycle of about 1% and with full focusing has a very high photoelectron peak current density. This could cause a degradation of performance due to space charge effects. Following the considerations of Lovergren and Massey[16,17], we estimate that we are close to the space charge limit at a spatial resolution of 10 nm with full refocusing of the OK-4/Duke UV FEL output. Less refocusing might be necessary, which might also prevent or reduce damage to the sample that could occur at the high power densities that are achieved with full refocusing.

3. Results

Initially the PEEM was operated with a Hg-arc laboratory source and for a limited time (60 hrs total) with spontaneous emission from the OK-4/Duke UV FEL. The outcoupling optics and the location of the PEEM at the Duke facility is shown in Fig. 5. This figure also shows the layout of the MBE system to be coupled to the PEEM microscope. Presently, a single mirror at the location labeled "periscope" in Fig. 5 is used to deflect the spontaneous emission of the OK-4 onto the sample. A lens supported on an X,Y, Z stage is used to refocus and steer the photon beam. Two other mirrors will be used to direct the lasing beam into the PEEM chamber. We will be able to alternately use photons generated in spontaneous emission or lasing mode. The low output power spontaneous emission will be utilized to identify the energy range most appropriate for a specific sample. Appropriate cavity mirrors and their tuning range can than be selected and installed for high output power, high spatial resolution *in-situ* dynamical studies. Since switching of cavity mirrors requires some time, being able to couple to the spontaneous emission will also allow utilization of shorter periods of operating time while unsuitable cavity mirrors are installed for FEL experiments other than the FEL-PEEM. In our first experiments, we have familiarized ourselves with and explored the various PEEM contrast mechanisms and PEEM operation during high temperature growth. In particular, threshold contrast changes with more than two surface phases was demonstrated, density of state contrast was observed, the question of information depth was addressed, and the extend to which samples with pronounced topography can be imaged was investigated. Initial results are presented which emphasize the value and effects of an FEL-PEEM system.

3.1. Spatial resolution and contrast changes due to photo-threshold differences: Cu(0.5ML)/ Mo(011)

Some of the highest spatial resolution to date with any PEEM has been achieved with Cu on Mo(011) samples [3]. Since pseudomorphic Cu and Mo(011) have workfunctions of 4.75 eV and 5.25 eV, respectively, these samples are convenient as they yield high contrast with a Hg laboratory source. In addition, the Cu decorates steps on the Mo(011) surface and small features can be produced with sub-monolayer Cu deposition. Prior to Cu deposition, the Mo(011) surface has been cleaned by decarborizing at T=1000°C for 10 hrs and removal of oxygen was achieved by flashing to T=1600°C several times during heating [18]. Cu was deposited at 550°C with a growth rate of 1 ML/40s. We show as an example of the high spatial resolution achieved with the PEEM a feature on a Cu/Mo(011) sample that has a width of 12 nm in Fig. 6. The actual spatial resolution of the instrument itself might be better, as we can not rule out that the feature width itself was near 12 nm. The measured feature width might be dominated by the sample, rather the instrumental broadening.

We have also utilized the same type of sample to explore contrast changes as a function of photon energy. In these experiments, the photon energy of the spontaneous emission of the OK-4 was varied in steps of 0.1 eV from 4.4 eV to 6.5 eV. We show, as example, the micrographs acquired at 4.4 eV, 4.6 eV, 5.1 eV, and 6.0 eV in Fig. 7. No attempt was made to achieve high spatial resolution in this particular experiment and the field of view is 50 μm for all images. The image at 5.1eV resembles most closely what is observed with the Hg-arc lamp. There seem to be two different types of morphological features; small dots and wavy lines. The following questions might be asked: what are the attributes that distinguish these features and are these features of the same composition. We obtain an indirect answer by comparing the images acquired at the different photon energies. Clearly, at 4.6 eV, only the dots emit strongly, while both features are "turned off" below the photo-threshold of both at 4.4 eV, and both features and the background emit relatively strongly at 6.0 eV. From this, we conclude that the photothreshold of the dots is lower than that of the wavy lines. Since Cu growth on Mo(011) is pseudomorphic, this difference is most likely not due to a difference in photo-threshold of two different Cu crystallographic orientations, but is rather due to compositional differences or a still contaminated interface. However, we can not exclude that 3-D growth resulted in a structure exposing a low workfunction surface of Cu, such as the (110) surface with a workfunction of 4.48 eV. Most likely however, insufficient removal of carbon contamination provides Cu growth nucleation centers that prevent the Cu from diffusing across the surface to decorate the Mo steps. The carbon contamination alters the photothreshold either directly by affecting the workfunction, or a carbon interface layer changes the band-lineup due to different Schottky barrier heights. Whatever the origin, these images show how the relative contrast between different sample regions can be manipulated by changing the incident photon energy, and how crossing the photothreshold of a feature turns this feature selectively on or off.

3.2. Density of states contrast: Pt silicides on Si(100).

We also investigated Pt silicides on Si(100) samples with the spontaneous emission from the OK-4 in steps of 0.1 eV. The samples were prepared external to the PEEM by depositing 5.0 nm of Pt onto Si(100) at room temperature. Annealing at 1000°C and subsequent data acquisition at room temperature was performed in the PEEM. Images acquired at 5.0 eV, 5.4 eV and 6.0 eV are presented in Fig. 9. The field of view in these images is 20 μm. All figures clearly show the presence of dots interpreted to be Pt silicides that self-organize during annealing. Closer inspection of Fig. 9 A reveals the presence of medium gray and bright grey dots in a dark background. When examining Fig. 9 B and particularly 9C, one can see that now the Si background is brighter than the medium gray features in

Fig. 9 A, while the brightest features tend to remain the brightest. Photothreshold, density of state and transport properties might all contribute to these observations. We will discuss these relative contributions in turn.

The possible composition of the two types of islands might be silicon-rich PtSi, PtSi, Pt_2Si, and Pt_3Si. The published workfunctions of Pt_2Si and PtSi are 5.17 eV, and 4.86 eV, respectively [19]. These values are close enough to be consistent with the possibility that the darker islands are Pt_2Si and the brighter islands are PtSi, even though we observe some emission of the "Pt_2Si" islands at 5.0 eV. Following the argument of Bethge and Klaua [11], who have observed photoemission from a Ni(110) surface with a nominal workfunction higher than the photon energy of the Hg-lab source utilized, we think that emission from the Pt_2Si is facilitated by a lowering of the workfunction by about 0.12 eV due to the Schottky effect in the presence of the 100,000 V/cm electric field. Given a photon energy width of 200 meV, at threshold energy of 5.05 eV would provide measurable emission from Pt_2Si islands at a nominal photon energy of 5.0 eV. Emission from a Pt_3Si phase, which would have a higher workfunction, would be very weak and unlikely, and Pt_3Si can be excluded as a possibility. Another possibility of producing islands of different composition might be that at the annealing temperatures utilized Si rich-PtSi and PtSi domains have been produced. This would result in two domains with different photothresholds that would both emit at the photon energies utilized. Even if the present tentative explanations regarding sample composition might not fully account for our observations and additional work to determine the photothreshold more precisely will be necessary, it is clear that not all dots are of the same composition. This aspect and the spatial distribution of each species could not be readily explored with AFM, a techniques that we have used previously to investigate silicide quantum dots [20].

The relative contrast changes between Fig. 9 A and in particular Fig. 9 C, are interesting and unique. Clearly, the contrast reversal between the darker round features and the background can not be due to the differences in photothreshold between the different surface phases. While differences in photothreshold can effect the relative contrast as the photon energy is varied, the brightest region, corresponding to the lowest photothreshold, should always be brightest, while the darkest should remain darkest if the photothreshold is the only variable effecting the relative contrast. We explore and discuss two possibilities that might explain the contrast reversal between two of the three phases: density of state and transport properties. Generally, the photo-yield depends on the density of states of the initial states and the final states above the photothreshold. Hence, our observation would require that the partial joint density of states of Si(100) corresponding to 6 eV is larger than the density of states in the silicides. The crossover in relative contrast is around 5.3 eV. An alternative explanation might be that the 6.0 eV photons penetrate the silicide and get absorbed deep inside the Si substrate.

On the way to the surface, excited electrons scatter much more strongly in the silicides than the Si and thermalize near the fermi level of the silicide and can not leave the surface due to the workfunction of the silicide. We calculate a penetration depth of about 3 nm for Pt for photon energies between 4 and 6 eV for 15° glancing illumination [21]. Given that the silicide islands after annealing are about 10-15 nm thick, it is very unlikely that a sufficient number of photons penetrate the silicide. In comparison, the penetration depth for Si at these energies is only half that of Pt. This indicates that the photo-yield might indeed be higher for Si than it is for Pt, even though the contribution of the conduction band density of states below the vacuum level to the short penetration depth of Si has not been assessed. Based primarily on the insufficient penetration of the silicide by the photons, we conclude that the observed contrast changes arise primarily from local differences in the density of state. The presented example underscores the advantages presented by a tunable photon source in order to explore relative contrast changes or even contrast reversal in a PEEM.

3.3. Sampling depth: Buried Ti contacts.

The use of wide bandgap semi-conducting materials has gained widespread interest due to their opto-electronic properties. Recent advances have produced blue LEDs and laser diodes. Along with these advances the issue of a reliable contact has become important. Cordes and Chang [22] have characterized the electrical properties of Ti contacts on MOVPE grown n-type GaN. Here we explore the possibility of characterizing the spatial variations of contacts by PEEM investigations of the Ti-AlN interface consisting of a Ti dot buried underneath 40 nm of CVD grown AlN. Assuming that the electron affinity of AlN is ~0 eV and the metal workfunction is 4.3 eV, the barrier to internal photoemission would be 4.3 eV within the Schottky-Mott model of the barrier. Photons with energies less than 6.1 eV should be able to deeply penetrate the AlN layer (AlN bandgap ~6.2 eV) and excite electrons at the Ti/AlN interface. Since the AlN surface has a negative electron affinity [23], all electrons excited into the conduction band and transported to the surface under the bias voltage are able to leave the surface and will be imaged with the PEEM. With tunable photons, the spatial variations of the band alignment at the interface might be probed.

Two samples were prepared; 25 nm thick, 100 μm diameter Ti dots were evaporated through a Mo screen directly onto a 6H-SiC substrate or onto an epilayer of GaN grown on a 0001 6H SiC substrate. A capping layer of 40 nm of undoped AlN was then grown over the Ti dots and substrate using CVD. The samples were investigated with the Hg-arc lamp as well as spontaneous emission from the OK-4 at various photon energies and temperatures. Preliminary results indicate that the dots

and their location can be identified in the images of the samples (See Figs. 10) as long as the photon energy is larger than about 4.5 eV. At 4.0 eV, essentially all contrast for the dots vanished, consistent with an "internal" photothreshold of about 4.3 eV (See for example, Fig. 10A). We also observe that the material grown without the GaN epilayer has significantly more features, which appear to be polishing scratches and other defects or imperfections. We are in the process of acquiring complementary information via SEM and AFM. Although our understanding of the features observed is incomplete, we again note that the relative contrast of features can be significantly effected by a change in photon energy. This rules out that the observations are a result of topographic contrast only. The results demonstrate a unique potential for examining buried interfaces.

3.5. Additional applications: Electron affinity of diamond surfaces

In diamond, different surface termination and adsorbate layers can induce a negative electron affinity [24-28]. Studies of diamond surfaces with the FEL-PEEM will be able to focus on the spatial variation of the relationship between surface morphology, growth conditions, adsorbate layers, and the photoemission and fieldemission properties. In initial experiments, the tunability of the OK-4/Duke UV FEL has allowed the direct observation of the change in photothreshold of diamond surfaces that occurs with the removal of the H termination layer. The diamond films (~ 1 micron thick) utilized for the PEEM experiment were prepared by plasma enhanced CVD. The film surfaces were subsequently hydrogen plasma cleaned for five minutes at an RF power of 20W, a Hydrogen pressure of 20 mTorr and a substrate temperature of 450°C. Shown in Fig. 12 are PEEM images of the H terminated diamond surface before and after annealing. The images were obtained with a photon energy of 5.6 and 6.0 eV, respectively. We observe that the hydrogen termination layer of the samples has been removed by annealing at a nominal temperature of 1000°C; the negative electron affinity surface was still emitting at 5.6 eV, while the surface without hydrogen termination did so to a much lesser extend. The relative difference in emission is most obvious when comparing the 5.6 eV images to those acquired at 6.0 eV. The photothreshold of the diamond surface was clearly increased due to the annealing. After establishing that 5.6 eV is a photon energy that can differentiate H terminated from un-terminated regions, we will be able to monitor the spatial variation of the H desorption process, its dynamics and dependence on temperature in future experiments.

We have also investigated several other samples and systems, including studies of the dynamics of growth and formation of Ti and Pt silicide islands, as well as the field emission properties of GaN pyramidal tips. Since these studies have not been performed with the OK-4/Duke UV FEL as a source, they have not been included here and will be reported separately.

4. Summary and future perspective

We have successfully completed the first test experiments with a high resolution PEEM coupled to the tunable OK-4 at the Duke FEL Laboratory. We have observed photothreshold and density of state contrast in images of several samples. These contrast mechanisms will be the most important ones to be exploited with a PEEM, and distinguishes the capabilities of a PEEM from those of LEEM. We have also successfully imaged deeply buried interface layers and strongly corrugated surfaces.

The Duke facility is in the process of completing the optics at the OK-4/Duke UV FEL that would allow us to couple the PEEM to the lasing output of the OK-4 rather than just to the spontaneous emission. In addition, the current of the electron storage ring will increase substantially over the currents utilized during the initial tests. This will provide a much higher photon flux at the sample and will allow real time, high spatial resolution imaging. We envision to perform a variety of experiments that range from growth of wide band gap semiconductors to surface processing issues and the dynamics of spinodal decomposition in polymer thin films.

Acknowledgments:

We acknowledge the excellent support and work of T. Franz and C. Koziol from Elmitec, the support of B. Müller and R. Guenther from Duke University, and the personnel at the Duke Free Electron Laser Laboratory for their help. Research at NCSU is supported by ONR under contract N00014-95-1-1141. The Duke FELL is supported by ONR contract N00014-941--0818 and AFOSR contracts F49620-93-1-0590, F49620-95-1-4076

Figure captions:

Fig. 1. Schematic of the PEEM.

Fig.2 Schematic layout of the Duke storage ring FEL facility. The 1 GeV Duke storage ring is driving variety of coherent and spontaneous light sources which are naturally phase-locked by the electron beam. The heart of the facility is the OK-4 FEL system which generates spontaneous radiation ranging from the IR to the soft X-ray range, coherent UV radiation and Compton back-scattered gamma-rays.

Fig. 3. Expected output power of the OK-4/Duke UV FEL for an average current of 100 mA. Expected extraction efficiency is between 25% and 80%, depending on the wavelength.

Fig. 4. Example of the spectral output of the OK4 in spontaneous emission mode with the peak centered at 5.75 eV.

Fig. 5. Layout of the PEEM coupled to the OK-4 (including the MBE to be installed).

Fig. 6. PEEM images of a Cu structure created during 1 ML deposited of Cu on Mo(011). A spatial resolution of 12 nm has been achieved. Field of view is 1.5 μm.

Fig. 7. PEEM images of structures form after deposition of 0.5 ML of Cu on Mo(011). Spontaneous emission from the Duke OK-4 was utilized: (a) 4.4 eV, (b) 4.6 eV, (c) 5.1 eV, and (d) 6.0 eV.

Fig. 8. PEEM images of Pt silicides imaged with the spontaneous emission from the OK-4 at a photon energy of: (a) 5.0 eV, (b) 5.4 eV, and (c) 6.0 eV.

Fig. 9. Ti dots on GaN epilayer under 40 nm of AlN utilizing spontaneous emission from the OK-4 of (a) 4.2 eV, and (b) 6.0 eV. Ti dots on SiC under 40 nm of AlN investigated with (c) Hg arc lamp, (d) OK-4 at 6.0 eV.

Fig.10. N-doped diamond thin film on Si after plasma cleaning. (a) $h\nu$ = 6.0 eV, no annealing, (b) $h\nu$ = 5.6 eV, no annealing, (c) $h\nu$ = 6.0 eV, after annealing, and (d) $h\nu$ = 5.6 eV, after annealing. Field of view of all images is 10 μm.

References:

[1]O.H. Griffith and W. Engel, Ultramicroscopy **36**, 1-28 (1991).

[2]W. Telieps and E. Bauer, Surf. Sci. **200**, 512 (1988).

[3]M. Mundschau, E. Bauer, and W. Swiech, Surf. Sci. **203**, 412-422 (1988).

[4]G.F. Rempfer, W.P. Skoczylas, and O.H. Griffith, Ultramicroscopy **36**, 196-221 (1991).

[5]L.H. Veneklasen, Ultramicroscopy **36**, 76-90 (1991).

[6]R.M. Tromp and M.C. Reuter, Ultramicroscopy **50**, 171-178 (1993).

[7]R.M. Tromp and M.C. Reuter, Phys. Rev. Lett. **68**, 821 (1992).

[8]A.W. Denier van der Gon, R.M. Tromp, and M.C. Reuter, Thin Solid Films **236**, 140-145 (1993).

[9]A.W. Denier van der Gon and R.M. Tromp, Phys. Rev. Lett. **69**, 3519-3522 (1992).

[10]This issue and references therein.

[11]H. Bethge and M. Klaua, Ultramicroscopy **11**, 207-214 (1983).

[12]H.H. Rotermund, W. Angel, M. Kordesch, and G. Ertl, Nature **343**, 355 (1990).

[13]G. Ertl, Surf. Sci. **299/300**, 742-754 (1994).

[14]V.N. Litvinenko, B. Burnham, J.M.J. Madey, S.H. Park, and Y. Wu, Nucl. Instr. Meth. Phys. Res. **A 375**, 46-52 (1996).

[15]V.N. Litvinenko, Report No. Duke FEL Report DFELL-1998-May-25, 1998.

[16]J.C. Lovegren and G.A. Massey, Microsc. Microanal. , 214-223 (1997).

[17]G.A. Massey, M.D. Jones, and B.O. Plummer, J. Appl. Phys. **52**, 3780 (1981).

[18]M. Mundschau and E. Bauer, J. Appl. Phys. **65**, 581 (1988).

[19]E. Bucher, S. Schulz, M.C. Lux-Steiner, P. Munz, U. Gubler, and F. Greuter, Appl. Phys. A **40**, 71-77 (1986).

[20]W. Yang, F.J. Jedema, H. Ade, and R.J. Nemanich, Thin Solid Films **308-209**, 627-633 (1997).

[21]E. Palik, (1985).

[22]H. Cordes and Y.A. Chang, MRS Internet Journal **2**, article 2 (1997).

[23]M.C. Benjamin, C. Wang, R.F. Davis, and R.J. Nemanich, Appl. Phyis. Lett. **64**, 3288-3290 (1994).

[24]F.J. Himpsel, J.A. Knapp, J.A.v. Vechten, and D.E. Eastman, Phys. Rev. B **20**, 624 (1979).

[25]F.J. Himpsel, D.E. Eastman, P. Heimann, and J.F.v.d. Veen, Phys Rev. B **24**, 7270 (1981).

[26]B.B. Pate, M.H. Hecht, C. Binns, I. Lindau, and W.E. Spicer, J. Vac. Sci. Technol. **21**, 364 (1982).

[27]B.B. Pate, Surface Sci. **165**, 83 (1986).

[28]J.v.d. Wide and R. Nemanich, Appl. Phys. Let. **62**, 1878 (1993).

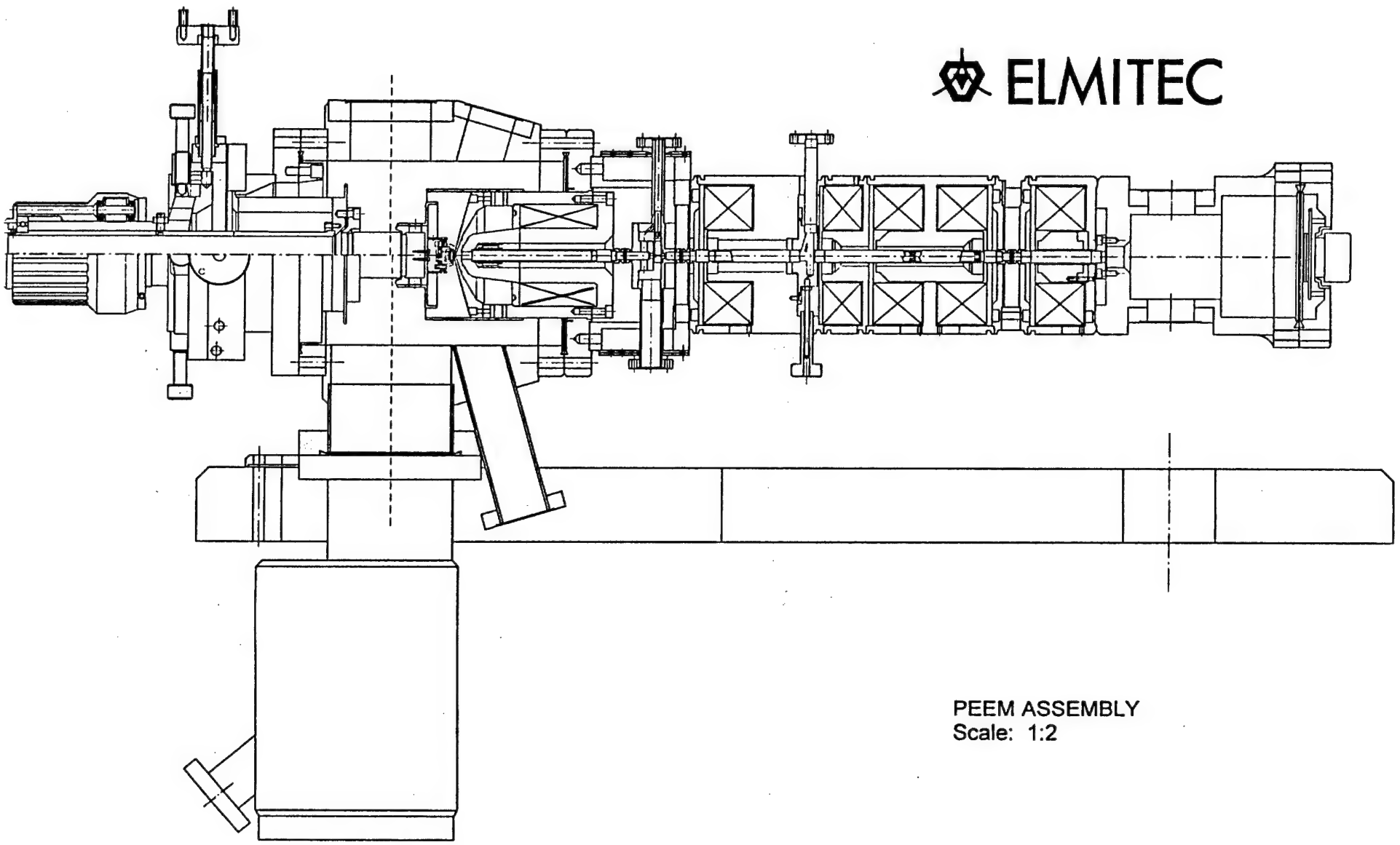

PEEM ASSEMBLY
Scale: 1:2

Fig 1 H. Acke et al.

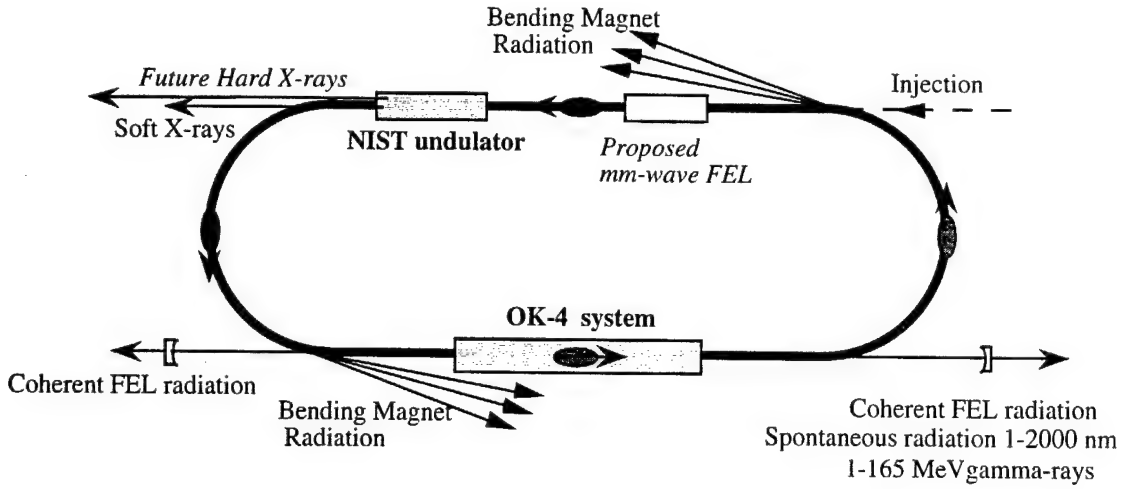

Fig. 2. H. Ade *et al.* "A Free…"

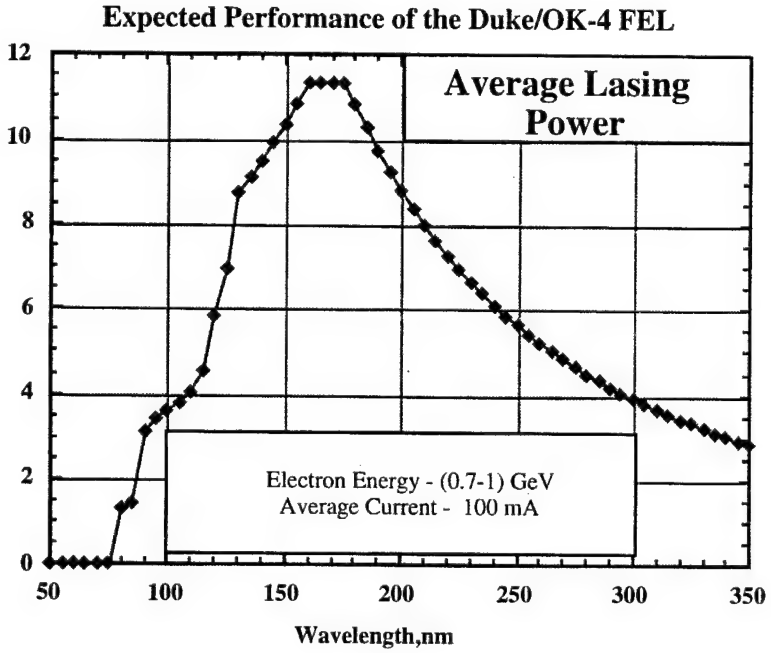

Fig. 3. H Ade *et al.* "A Free…."

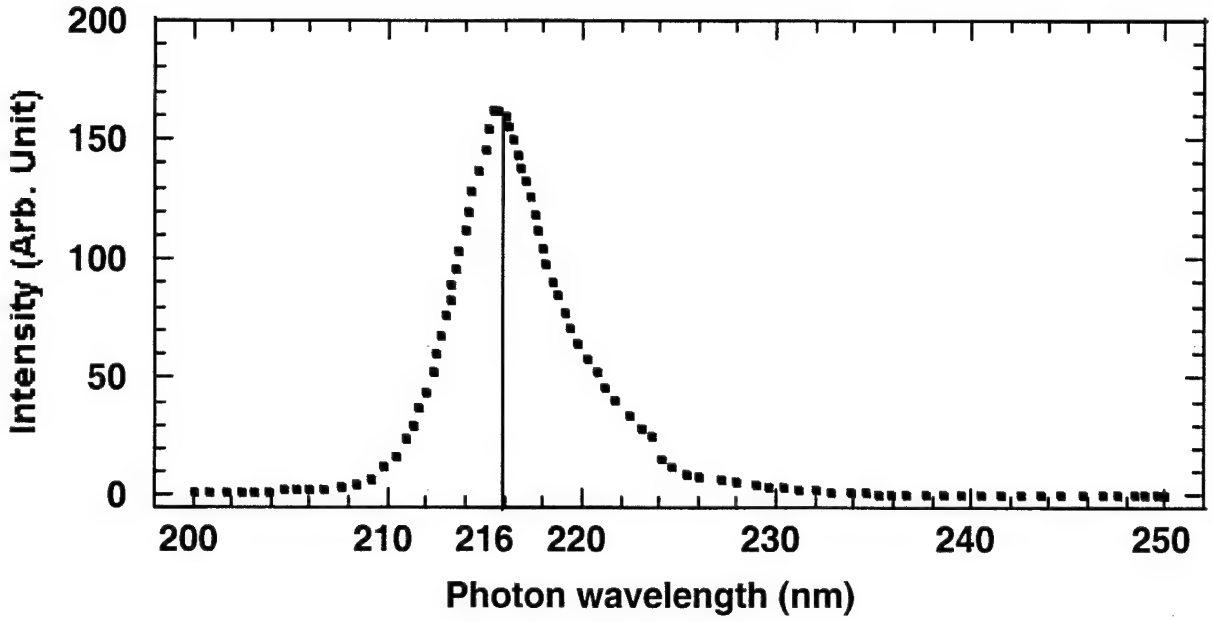

Fig. 4 The spectral output of the OK-4 in spontaneous emission mode with the peak centered at wavelength of 216nm

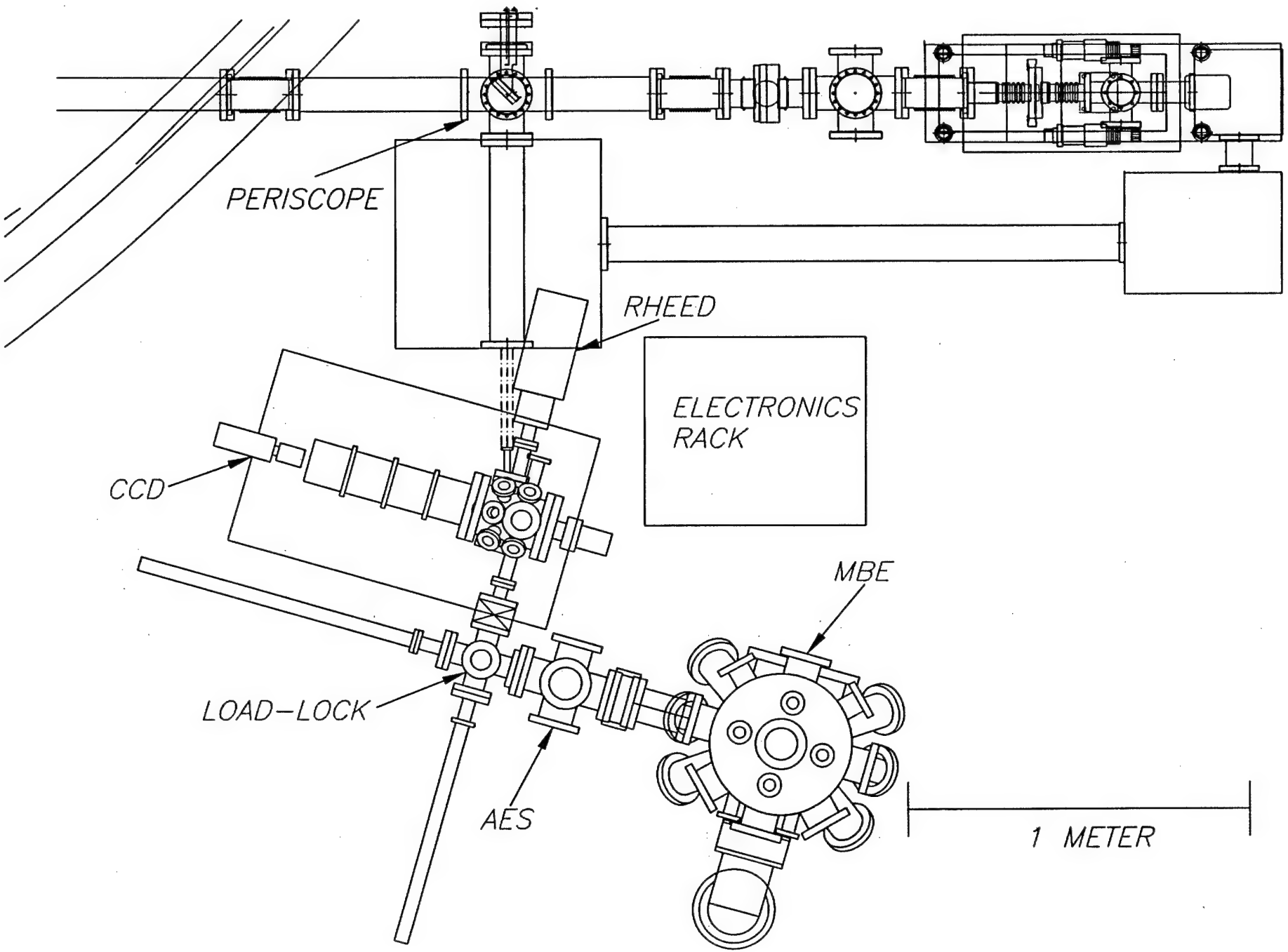
PERISCOPE
RHEED
ELECTRONICS RACK
CCD
MBE
LOAD–LOCK
AES
1 METER

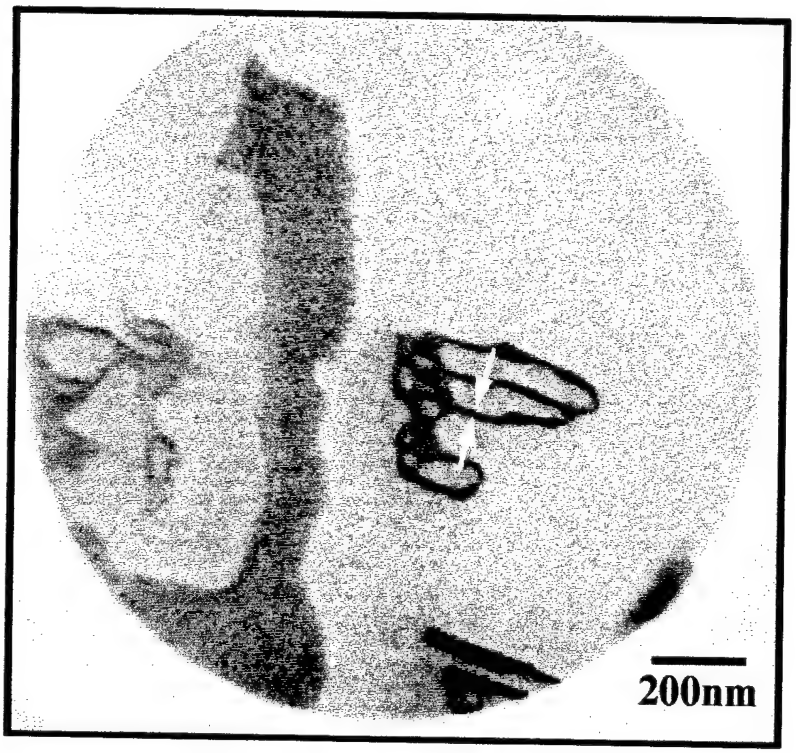

Fig. 6 PEEM image of 1ML Cu deposition on MO(110). The lateral resolution of image is ~10nm. The field of view is 1.5um.

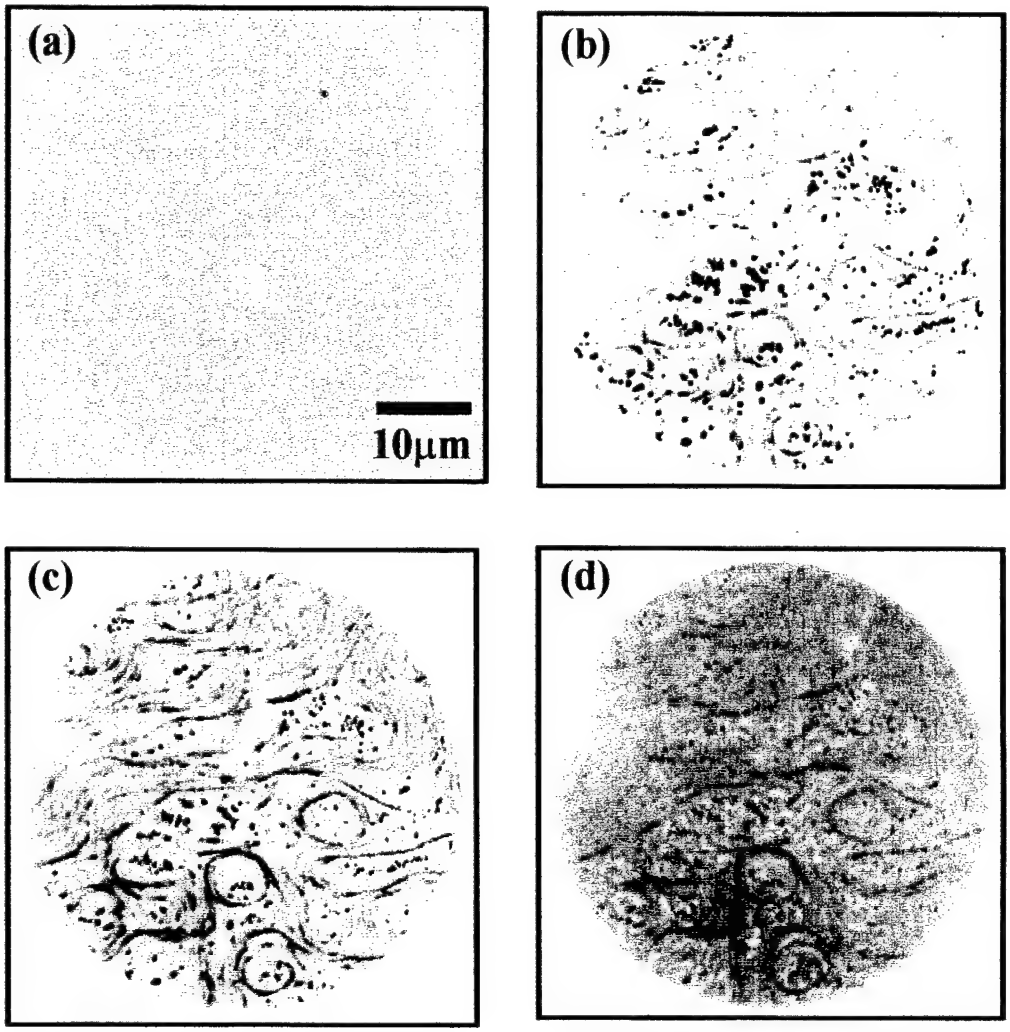

Fig. 7 PEEM images of 0.5ML Cu deposition on Mo(110) surface with varying photon energy of OK-4 FEL (a) 4.4eV (b) 4.6eV (c) 5.1eV (d) 6.0eV

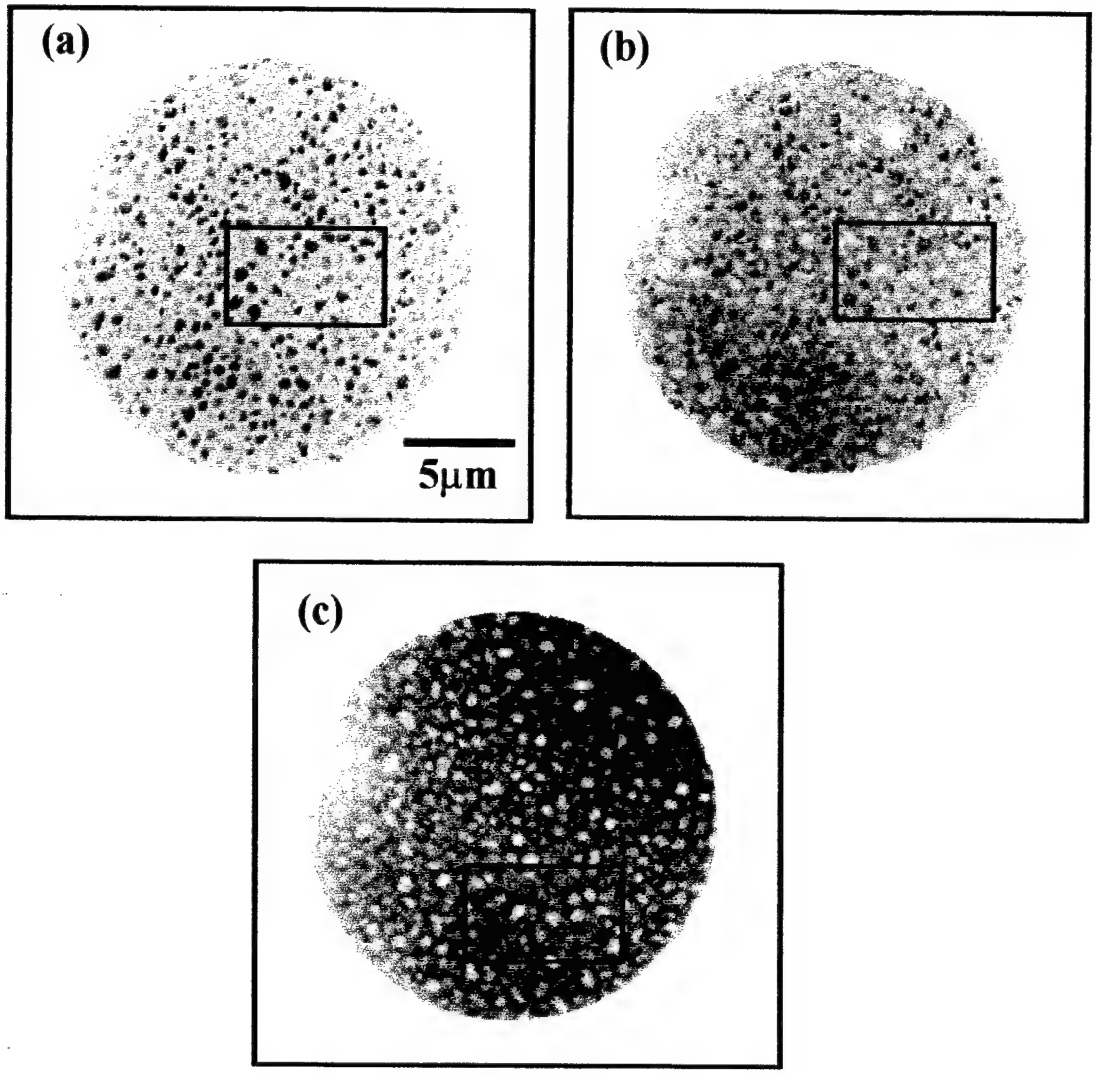

Fig. 8 PEEM images of Pt silicides with varying photon energy of OK-4 FEL
(a) 5.0 eV (b) 5.4eV (c) 6.0eV

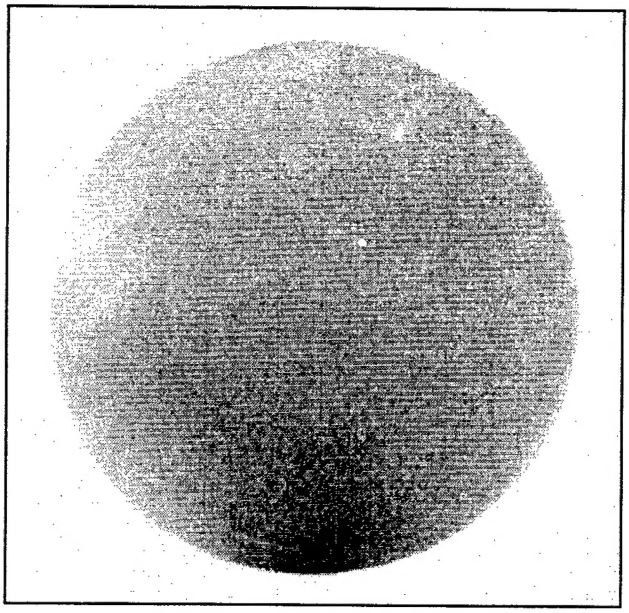

Figure A

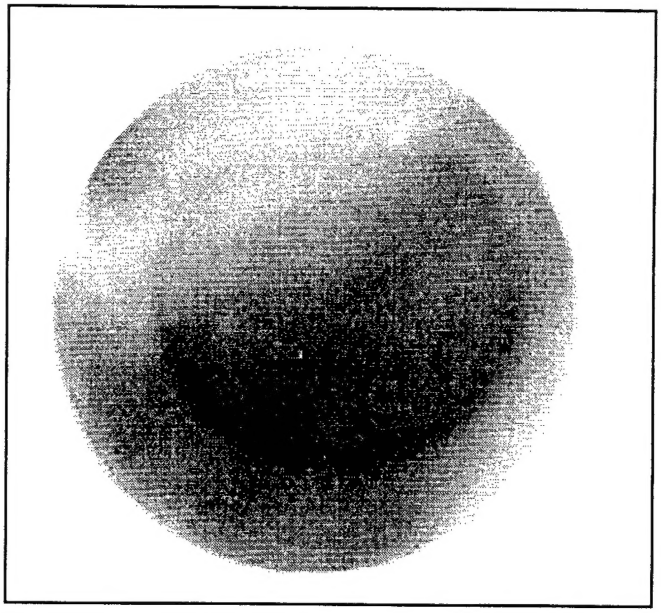

Figure B

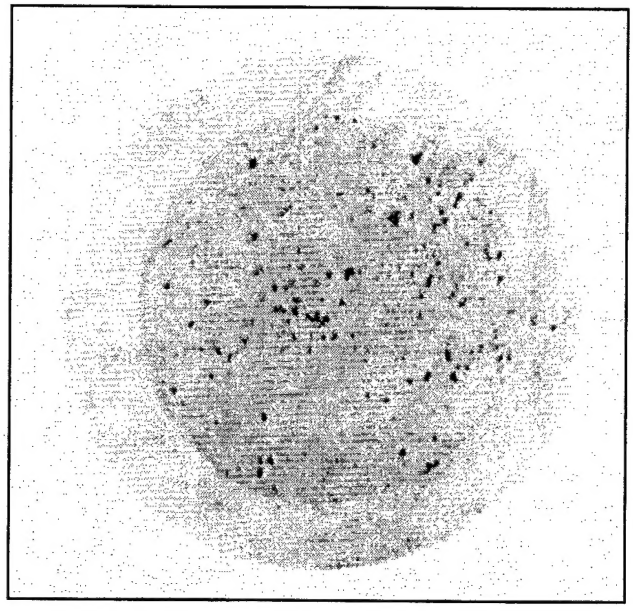

Figure C

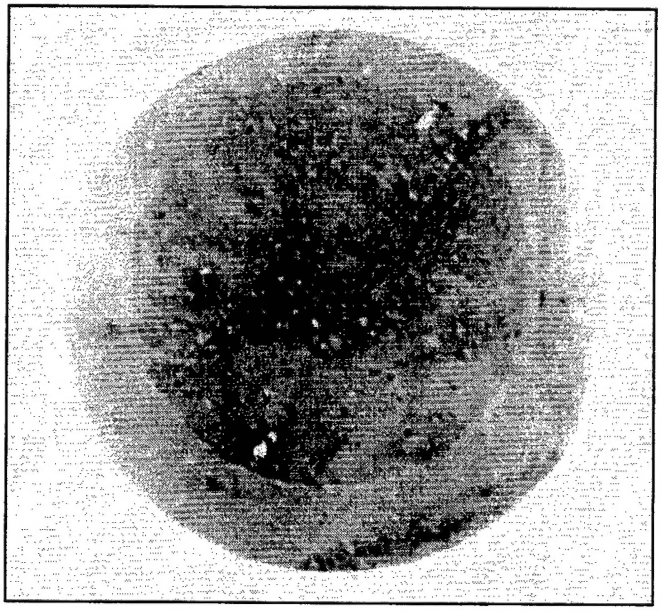

Figure D

FIGURE 9

N-doped Diamond Thin Film on Si
after H plasma cleaning
10μm field of view
taken at Room Temperature

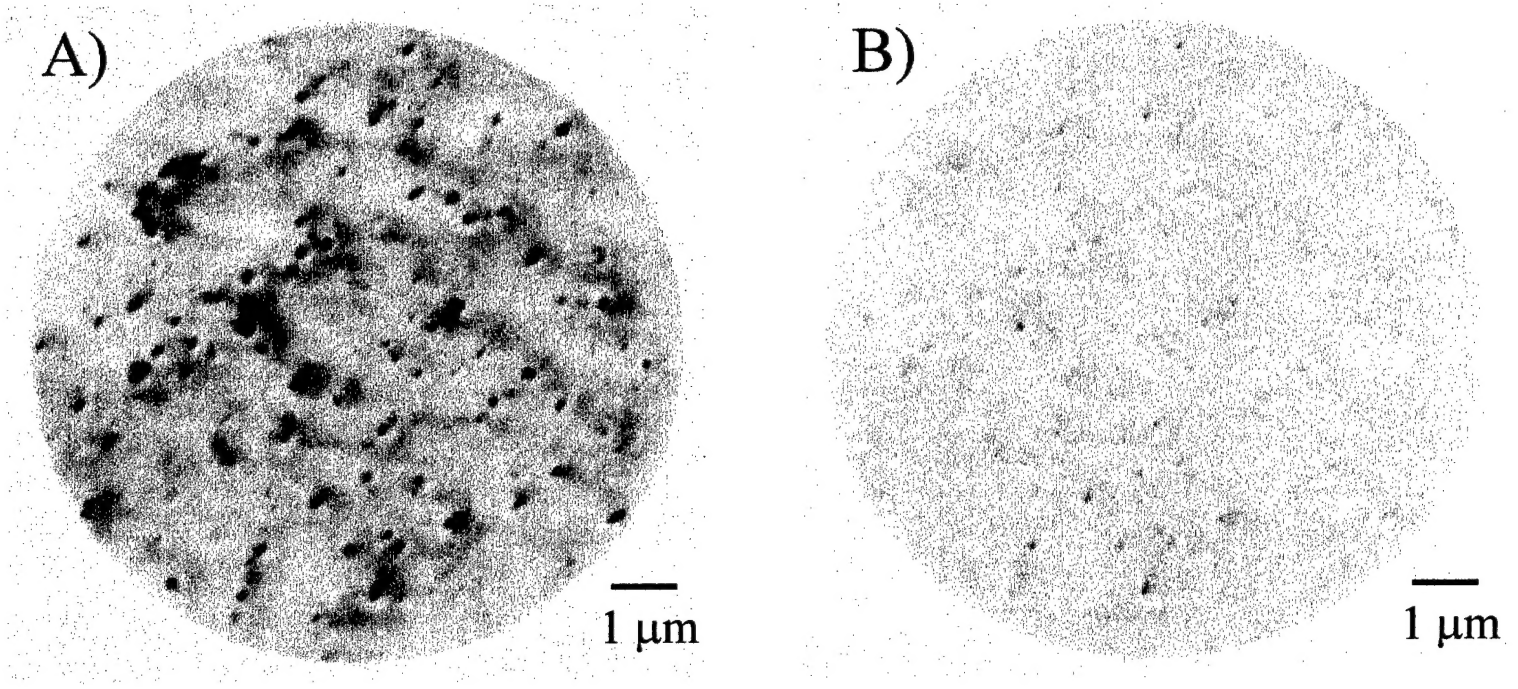

hν = 6.0 eV

hν = 5.6 eV

FIGURE 10

N-doped Diamond Thin Film on Si
after H plasma cleaning
10μm field of view
taken after 1000° C (10 min)

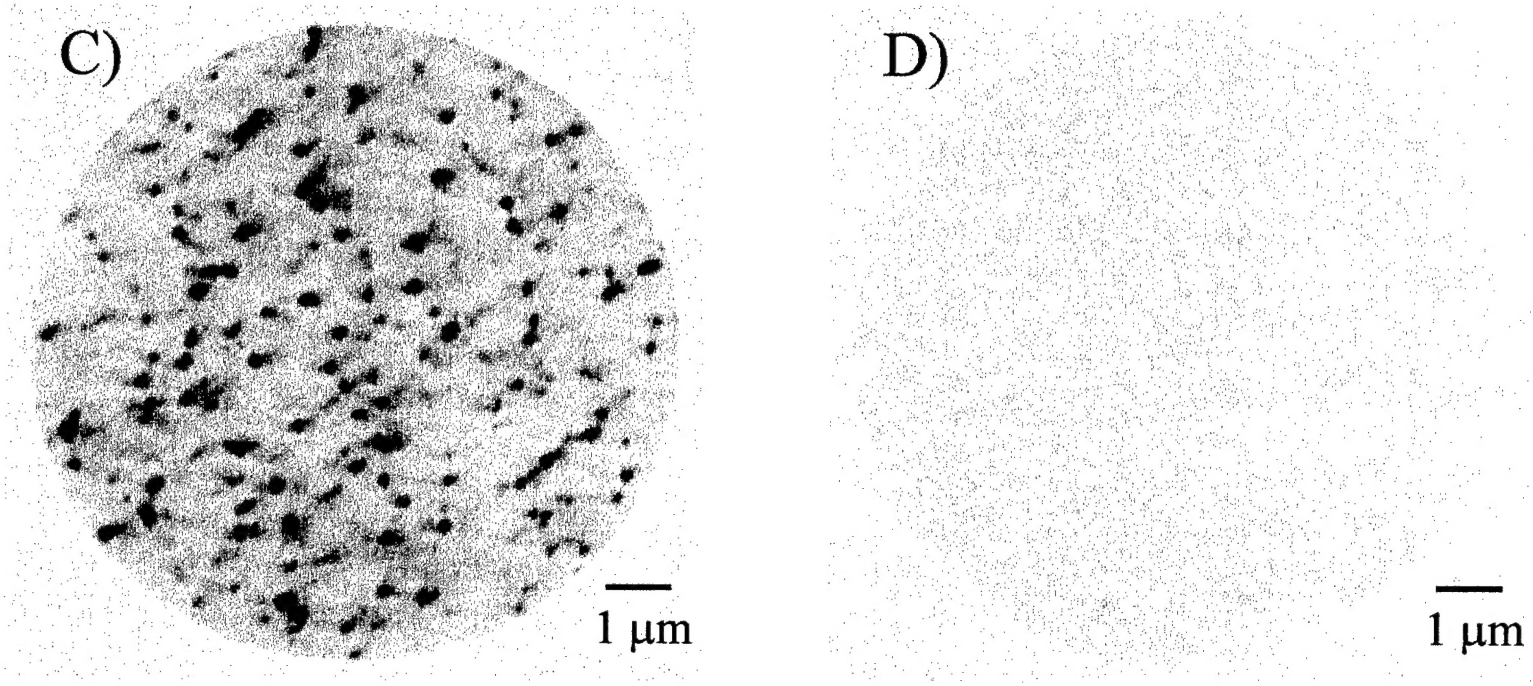

hν = 6.0 eV

hν = 5.6 eV

FIGURE 10

Distribution List	Number of Copies
Program Manager/Officer ONR: 312 Larry R. Cooper Office of Naval Research Ballston Tower One 800 North Quincy Street Arlington, Virginia 22217-5660	3
Administrative Grants Officer Office of Naval Research Regional Office Atlanta 101 Marietta Street, Suite 2805 Atlanta, GA 30323-0008	1
DIRECTOR, Naval Research Laboratory ATTN: Code 2627 Washington, DC 20375	1
Defense Technical Information Center Building 5, Cameron Station Alexandria, Virginia 22304-6145	2
Office of Naval Research Ballston Tower One ATTN: ONR OOCC1 Mr. William F. McCarthy 800 North Quincy Street Arlington, Virginia 22217-5660	1